



A novel highly reactive Fab antibody for breast cancer tissue diagnostics and staging also discriminates a subset of good prognostic triple-negative breast cancers



Thaise G. Araújo^a, Carlos E. Paiva^b, Rafael M. Rocha^c, Yara C.P. Maia^a, Angela A.S. Sena^a, Carlos Ueira-Vieira^a, Ana Paula Carneiro^a, Juliana F. Almeida^a, Paulo R. de Faria^d, Donizeti W. Santos^e, Luanda Calábria^e, Tânia M. Alcântara^f, Fernando A. Soares^c, Luiz R. Goulart^{a,g,*}

^a Federal University of Uberlândia, Institute of Genetics and Biochemistry, Nanobiotechnology Laboratory, Campus Umuarama, Bloco 2E, Sala 248, 38400-902 Uberlândia, MG, Brazil

^b Division of Breast and Gynecological Tumors, Department of Clinical Oncology, Barretos Cancer Hospital, Barretos, SP, Brazil

^c AC Camargo Cancer Hospital, São Paulo, SP, Brazil

^d Federal University of Uberlândia, Biomedical Sciences Institute, Uberlândia, MG, Brazil

^e Obstetric Division, Internal Medicine, University Hospital, Federal University of Uberlândia, Uberlândia, MG, Brazil

^f Pathology Division, Internal Medicine, University Hospital, Federal University of Uberlândia, Uberlândia, MG, Brazil

^g University of California Davis, Dept. of Medical Microbiology and Immunology, Davis, CA, USA

ARTICLE INFO

Article history:

Received 28 January 2013

Received in revised form 26 September 2013

Accepted 26 September 2013

Keywords:

Phage display
Recombinant antibody
Combinatorial library
Breast cancer

ABSTRACT

The discovery of novel markers for breast cancer (BC) has been recently relied on antibody combinatorial libraries and selection through phage display. We constructed a recombinant Fab library, and after selections against BC tissues, the FabC4 clone was thoroughly investigated by immunohistochemistry in 232 patients with long-term follow-up. The FabC4 ligand was determined by mass spectrometry. The FabC4 expression was associated with younger age, lack of progesterone receptor, higher histological grades and non-luminal subtypes, and it also identified a subset of good prognostic triple-negative BCs, possibly targeting a conformational epitope of Cytokeratin-10 (CK10). This new CK10-epitope specific antibody may open new possibilities in diagnostic and therapeutic strategies.

© 2013 Elsevier Ireland Ltd. All rights reserved.

1. Introduction

Breast cancer (BC) is the most frequent malignant tumor of women in North America [1], is the second leading cause of death, after lung cancer [2] and the parameters currently available are not sufficient to capture its individual complexity [3]. During the past decade, several genomics-based techniques have significantly improved the molecular characterization of breast tumors, and these approaches have expanded the BC classification, which resulted in new clinical diagnostic tests [4]. However, the heterogeneous nature of this disease, encompassing a wide variety of pathological entities in which 40% of the patients still succumb, highlights the need for new therapeutic strategies and identification of new targets [3,5].

It is known that malignant transformation of cells often causes dramatic changes in the expression of cell surface molecules [6], and antibodies have proven to be excellent high-affinity protein-based ligands to detect such alterations [7]. Antibody therapy offers great promise for cancer treatment, and several antibodies have been approved in clinical settings. Among them, the anti-HER-2 extracellular domain humanized monoclonal antibody, trastuzumab, is considered to be the prototype of a successful target drug. It has been widely used in the last decade for the treatment of HER-2 positive BCs in the neoadjuvant, adjuvant and metastatic settings [8–10].

Monoclonal antibodies (mAb) are generated by either hybridoma or by combinatorial antibody technologies [6], with libraries that can be naïve, semi-synthetic, synthetic and fully synthetic [11]. Recombinant antibodies present several advantages, such as: production in recombinant bacteria, yeast or plant, immunization is not required, and intrinsic properties such as immunogenicity, affinity, specificity and stability can be improved by various mutagenesis technologies [12]. Thus, the construction and selection of antibody combinatorial libraries expressed on filamentous

* Corresponding author at: Federal University of Uberlândia, Institute of Genetics and Biochemistry, Nanobiotechnology Laboratory, Campus Umuarama, Bloco 2E, 38400-902 Uberlândia, MG, Brazil. Tel.: +55 34 3218 2478; fax: +55 34 3218 2203.
E-mail address: lrgoulart@ufu.br (L.R. Goulart).

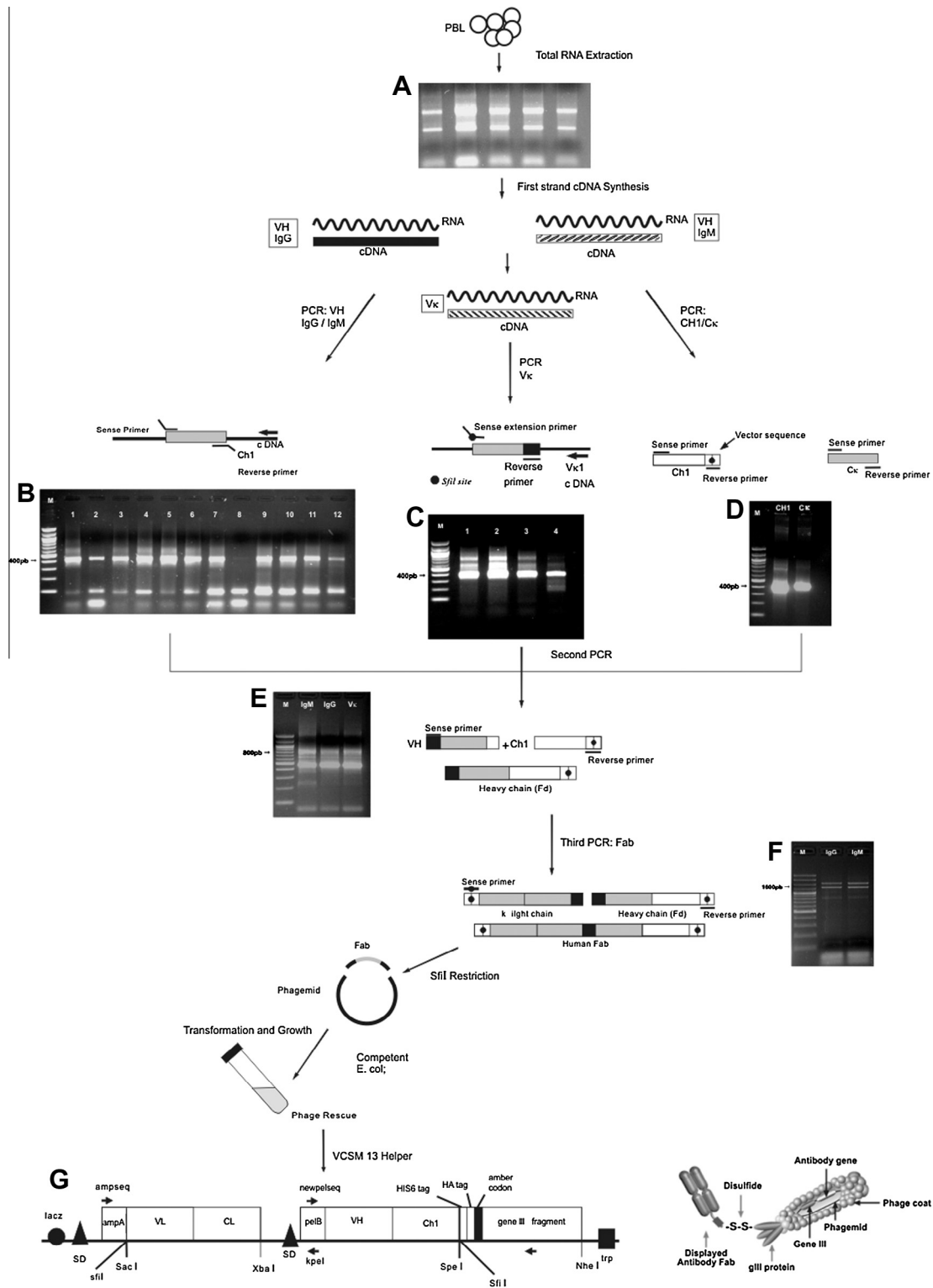


Fig. 1. Schematic outline of the construction the Fab repertoire using phage display. Total RNA was first isolated (A) and IgG and IgM heavy chain were amplified including five VH families (B) followed by Vκ (C), CH and Cκ (D) amplifications. The purified amplicons were assembled in a second round of PCR (E) which was assembled to generate the human Fab fragment (F). After *SfiI* digestion and ligation of the Fab to the phagemid, the ligated vector was induced into *E. coli*. The culture was infected by VCSM13 helper and displayed as fusion to pIII coat protein.

phage surface became an important strategy to search for novel antigen-specific ligands with higher affinity and without cross-reactivity, due to their unequal, expanded and diverse antibody repertoire, with important applications in diagnosis and therapy [8–10].

The selected phage displayed antibody combinatorial fragments mimic immune selection and maturation of antibodies, providing the most robust, versatile and wide spread selection method in the past decade [11,13]. A crucial advantage of this technology is the direct link between the experimental phenotype and its

Table 1
Patients' characteristics (N = 232).

Variable	Patients	
	N.	%
<i>Age (years)</i>		
Median (range)	54	(25–86)
<i>Menopausal status</i>		
Premenopausal	98	42
Postmenopausal	134	58
<i>Lymph node status</i>		
cN0	74	32
cN1–3	158	68
<i>Tumor stage</i>		
cT1	19	8
cT2	101	43
cT3	48	21
cT4	64	28
<i>Histological grading</i>		
G1	44	19
G2	127	55
G3	61	26
<i>ER status</i>		
Negative	84	36
Positive	134	58
NA	14	6
<i>PgR status</i>		
Negative	156	67
Positive	65	28
NA	11	5
<i>HER-2^a</i>		
Negative	166	72
Positive	22	9
NA	44	19
<i>Breast cancer subtypes^b</i>		
Luminal	148	64
HER-2-enriched	16	7
Triple negative	48	21
NA	20	8
<i>Chemotherapy</i>		
No	39	17
Yes	193	83
<i>Radiation therapy</i>		
No	39	17
Yes	193	83
<i>Hormone therapy</i>		
No	126	54
Yes	106	46

Abbreviations: NA = not available; ER, estrogen receptor; HER2, human epidermal growth factor receptor 2; PgR, progesterone receptor.

^a HER2 status was considered as positive (score 3+) and negative (score 0–1+); scores 2+ were excluded from the analyses.

^b Cases were classified as luminal (ER+ and/or PgR+ with HER-2-), HER2-enriched (ER-/PgR-/HER2+), and triple negative (ER-/PgR-/HER2-).

encapsulated genotype, which allows the evolution of selected binders into optimized molecules [14,15], as shown against different antigens [12,13,16,17], including melanoma [18], colorectal [19] and prostate [6,20,21] cancer proteins.

In this study, we have constructed a Fab combinatorial antibody library on M13 phage from transcripts of BC patients. The choice of the Fab format was based on the notion that monomeric appearance of the Fab permits the rapid screening of large numbers of clones [16]. Additionally, Fab antibodies are more stable and amenable to retaining the natural folding and binding characteristics, governed by affinity rather than avidity, avoiding such problems presented in multimeric scFv libraries [21]. While genetic and epigenetic changes in genes that regulate mammary epithelial cell proliferations, survival, polarity and/or differentiation are probable initiators of breast carcinogenesis, several lines of evidence

indicate that stromal cell responses may promote cancer progression and metastasis [22]. To identify these probable factors involved in BC development in stromal cells, we have analyzed the library diversity, and selected a target-specific antibody clone, FabC4, against antigens from tumor breast tissues. Its applicability in a cohort of BC patients with long-term follow-up was evaluated in order to associate its expression with clinical-pathological characteristics and survival.

2. Materials and methods

2.1. Study design and sample collection for library construction

This Project was carried out from 2008 to 2009 at the Nanobiotechnology Laboratory of the Federal University of Uberlândia (UFU) together with the Obstetrics' Services of University Hospital. The study protocol was approved by the UFU Research Ethics Committee (N. 176/2008), and an informed consent was obtained from all participants. All peripheral blood leukocytes (PBL) and tissue samples were obtained from patients that live in Uberlândia – MG (Brazil). The ethnic background was not recorded since the Brazilian population is highly heterogeneous and mixed. Peripheral blood samples were collected before surgery in a vacutainer™ tube containing K₂EDTA 7.2 mg, and maintained at 4 °C.

To construct the Fab combinatorial library, we have obtained PBL from 20 women patients (mean age of 54 years) with ductal invasive BC grade I (5%), grade II (90%) and grade III (5%), submitted to mastectomy with no preoperative chemotherapy, radiation or hormonal therapy. Breast tissues from three patients diagnosed with ductal invasive BC (two classified as grade II and one as grade III, mean age of 52 years, mastectomized, and presenting more than 80% of malignant tissue) were used to perform selection of the phage displayed antibody library. Normal tissues from patients submitted to breast reduction surgery (mean age, 50 years), and with no familial history of breast cancer, were collected under an informed consent and were classified as a control group.

2.2. RNA extraction and first-strand cDNA synthesis

Total RNA was extracted from PBL of each patient by Guanidine Isothiocyanate extraction method [23] with minor modifications. The RNA concentration and quality were analyzed in a 1.2% agarose gel electrophoresis stained with ethidium bromide and by absorbance readings at 260 and 280 nm. RNAs were pooled in equimolar concentrations and used to synthesize the first-strand cDNA. Four micrograms of this RNA pool were mixed with 10 pmol of specific primers for amplifications of the heavy and light chain immunoglobulins [22] that were submitted to 70 °C for 10 min. The reverse transcription was performed with 10U of SuperScriptII Reverse Transcriptase (Invitrogen), 5X SuperScript-RT Buffer, 10U of RNase inhibitor (Invitrogen) and 200 μM of each dNTP, which was incubated at 42 °C for 60 min. The reaction was terminated by heating at 70 °C for 15 min.

2.3. Construction of human Fab combinatorial library

First-strand cDNA derived from PBL of BC patients was used to generate the Fab genes repertoire by PCR reactions as described elsewhere [26]. Briefly, two sets of six PCR amplifications were performed by using sense primers for VH fragments, combined with g or m anti-sense primers. Similarly, VL gene fragments were obtained by using four sense primers, covering the whole kappa repertoire. These primers were used with a single 3' oligonucleotide targeting the kappa constant region (Cκ). Primers used in this first PCR reaction were designed for the posterior assembly of the heavy chain (Fd) fragment in a second PCR reaction. For this purpose, g and m VH fragments were fused to a g constant region (CH1). The complete light chains were constructed by fusing VLs to a Cκ fragment in another PCR reaction. Fd fragments and kappa light chains were ultimately shuffled in a final overlap recombinant PCR. Cloning procedures, preparation of phage and the construction of the Fab library were performed as described elsewhere [24], and demonstrated in Fig. 1.

2.4. Library size

A total of 7.4 μg of DNA was electroporated into the XL1-Blue *E. coli* strain to generate the Fab phage library. After electroporation, the cuvette was flushed with 3 mL of SOC medium (contains bactotryptone, bacto yeast, NaCl, KCl, MgCl₂ and glucose) and transformed cells were incubated for 1 h at 37 °C before spreading on LB agar/carbenicillin (50 μg/mL) plates. Then, the plate was incubated overnight at 37 °C. The size of the library was determined by 10-fold serial dilutions of the transformed cells.

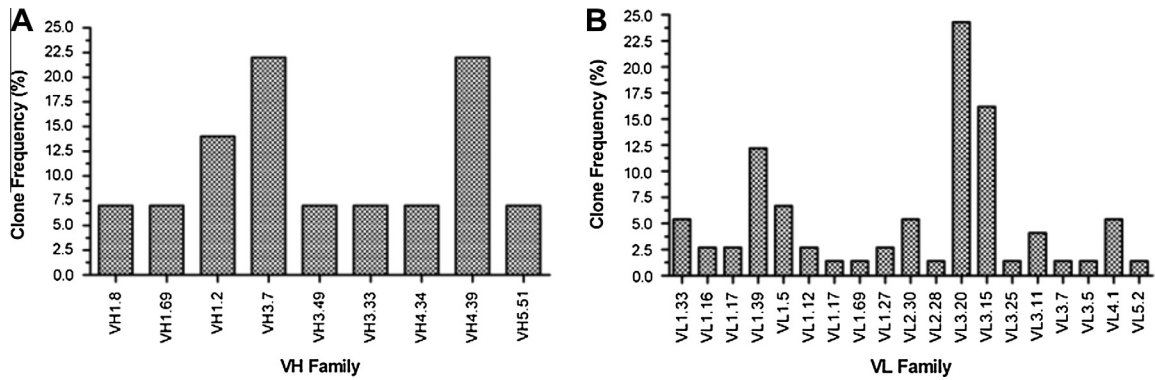


Fig. 2. VH and VL repertoire of non-amplified original Fab library. The graph shows the frequency of VL (A) and VH (B) gene segment family usage (%). The sequences were aligned to their closest germline, using the Ig-Blast to identify the V family.

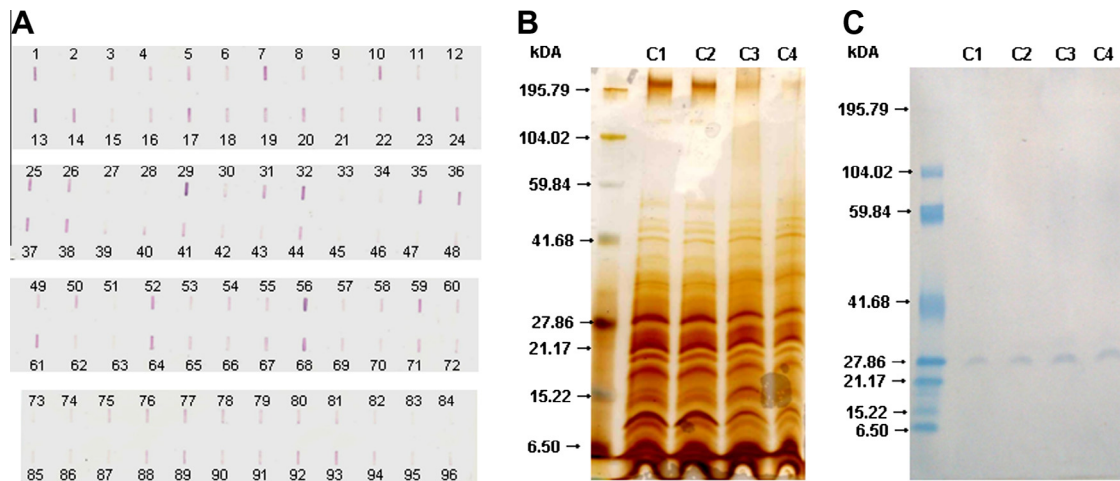


Fig. 3. Characterization of selected clones after induction by IPTG. The presence of soluble Fab fragments was evaluated by anti-HA antibody, which recognized the hemagglutinin tag fused to VH chain. Slot blot analysis demonstrated Fab expression in 98% of selected clones (A). Clone 84 corresponds to pCom3X vector supernatant without Fab fragment. SDS-PAGE (B) and Western-Blot assays (C) was performed to confirm the presence of human Fab in culture supernatants which corresponds to ~28 kDa. M shows Prestained SDS-PAGE Standards, Broad Range (Bio-Rad) and C1–C4 shows randomly selected clones from expression plates.

2.5. Antibody selection by phage display

Selection of phage particles displaying specific Fab fragments was performed directly in fresh tissues, right after the surgery. The subtractive selection was performed in tissues from patients submitted to mastectomy, neither with benign mammary disease nor with familial history of BC. For each round of selection, phage particles were amplified. For this purpose, 50 μ L of XL1-Blue electrocompetent cells were inoculated in 50 mL of super broth (SB) medium containing tetracycline (10 μ g/mL). The culture was shaken until $OD_{600nm} = 1.0$ and infected by 50 μ L of phage display antibody library incubated 1 h at 37 $^{\circ}$ C. The infectious phage titer was determined by adding 1 μ L and 10 μ L on *E. coli* culture in Luria Broth supplemented with 20 μ g/mL of carbenicillin and 2% glucose, which were shaker-incubated at 37 $^{\circ}$ C for 16 h. The carbenicillin concentration was then increased to 50 μ g/mL. After an additional 1-h incubation at 37 $^{\circ}$ C, cultures were centrifuged at 3000 \times g for 10 min at room temperature and resuspended in 500 mL of pre-warmed SB medium supplemented with tetracycline and carbenicillin, as previously described, and 2 mL of VCSM13 helper phage ($>1 \times 10^{12}$ PFU/mL). After 2-h incubation at 37 $^{\circ}$ C, cultures were supplemented with 70 μ g/mL of kanamycin, and further incubated overnight at 37 $^{\circ}$ C. The phages were precipitated as previously described, and used in the next selection cycle, following a total of three rounds of selection. After the third cycle, selected colonies were amplified and induced for soluble production of Fab, followed by phagemid DNA extraction. For each selection cycle, normal tissues were placed in a microtube containing 1X PBS (phosphate-buffered saline) until processing. After washing with PBS/2% BSA, tissues were incubated with 50 μ L of amplified library with PBS/2% BSA in a final volume of 500 μ L, and incubated at 4 $^{\circ}$ C for 1 h. The unbound phages in the supernatant were transferred to a microtube with a fresh microdissected breast cancer tissue with the addition of Tween-20 to a final concentration of 0.05%, and

incubated at 4 $^{\circ}$ C for 2 h. The unbound viral particles were discarded, and the tumor tissue was washed 10 times with PBST (PBS/Tween-20 0.1%) by centrifugation at 3000 \times g for 2 min. The bound phages were submitted to a competitive elution transferring the tissue to an XL1-Blue electrocompetent bacterial culture in $OD_{600nm} = 1.0$ for infection, phage amplification and titration.

2.6. Soluble Fab antibodies production

Individual selected clones from the third selection round were grown overnight at 37 $^{\circ}$ C in deep-well plates containing 1 mL of SB medium supplemented with 50 μ g/mL carbenicillin and 2% glucose in each well. Phagemids without Fab inserts were grown in two wells, as negative controls. In a new deep-well plate containing supplemented SB medium, 50 μ L of each clone was transferred and incubated by shaking at 37 $^{\circ}$ C. After reaching the absorbance (OD_{600}) equal to 1.0, the culture was centrifuged at 3000 \times g for 10 min at 4 $^{\circ}$ C. Bacteria were resuspended in 1.5 mL SB medium and induced with 2.0 mM IPTG overnight at 30 $^{\circ}$ C (no more than 18 h). The supernatant containing the Fab was obtained by 3000 \times g centrifugation for 20 min and was directly subjected to Immunoblot and ELISA analyses.

2.7. Slot-blot, SDS-PAGE and Immunoblot

Slot-blot analysis was performed using the induced culture supernatants of randomly chosen selected clones. Ten microliters of each selected clone supernatant was applied to a nitrocellulose membrane (Hybond ECL, Amersham Biosciences). The membrane was dried at room temperature, blocked with BSA3% (w/v) in PBS for 1 h at room temperature and washed 3 times with PBST 0.05%. The soluble anti-body was detected with 1:5000 diluted HRP-conjugated rat anti-HA (Roche Applied

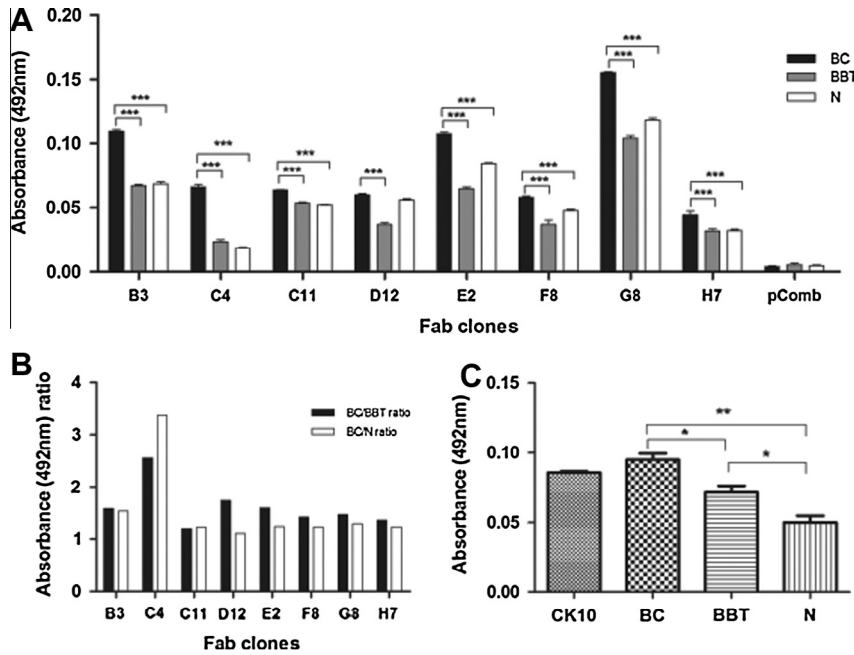


Fig. 4. Evaluation of the binding selectivity of the induced clones using a pre-screening ELISA in total protein extracted from normal, benign and tumor tissue samples. Absorbance in 492 nm is described in panel A with 8 reactive clones obtained from supernatant of bacterial medium after IPTG induction. ANOVA test demonstrated that all clones discriminated breast cancer from benign samples. FabC4 clone was selected for additional procedures, based on its reactivity ratio between cancer/benign and cancer/control (B), which was higher than the other clones. ELISA assay between the recombinant CK10 and the FabC4 antibody for antigen validation (C). Absorbance was significantly different between the three groups of proteins extracted from BC; BBT and N patients. BC protein did not differed from CK10 absorbance and was positive for HPLC-purified FabC4 detection. The other groups presented significantly lower absorbance compared to CK10 recombinant protein. BC: breast cancer; BBT: benign breast tumor; N: normal tissue. **P* < 0.05; ***P* < 0.01; ****P* < 0.001.

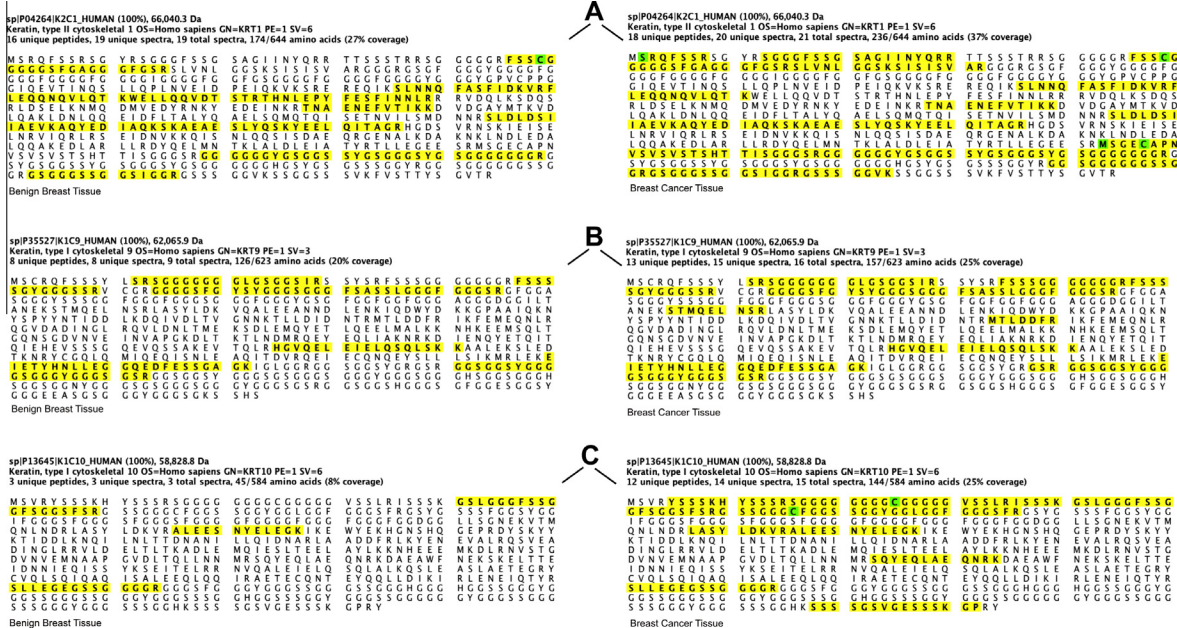


Fig. 5. Mass spectrometry sequencing for FabC4 target detection comparing breast cancer and benign tissues. It was detected three potential targets: CK1 (A), CK9 (B) and CK10 (C). According to peptide matches and comparing the two groups CK10 was characterized as FabC4 target. In yellow: peptide matches. (For interpretation of the references to color in this figure legend, the reader is referred to the web version of this article.)

Science), since pComb3X vector contains a hemagglutinin (HA) tag for immunodetection. After 2 h of incubation at room temperature the membrane was washed with PBST and visualized using 3,3'-diaminobenzidine (DAB) (Sigma Aldrich). In order to confirm the presence of Fab fragments, four clones were randomly selected, and 30 µL of the supernatant were separated by 12.5% SDS-PAGE and blotted onto 0.22 µm nitrocellulose membrane for Western Blot analysis, which was performed according to the slot-blot assay.

2.8. ELISA screening of selected clones

In order to investigate BC antigen recognition, Immuno 96 Micro-Well™ (Nunc, Denmark) plates were coated with 1 µg/well of total protein extracted from pools of normal, benign and tumor breast tissues in 100 µL of sodium bicarbonate buffer pH 7.4 (NaHCO₃), at 4 °C overnight. The plates were washed 3 times with PBST 0.05% and blocked with 5% slim milk-PBS for 3 h at room temperature. After washes,

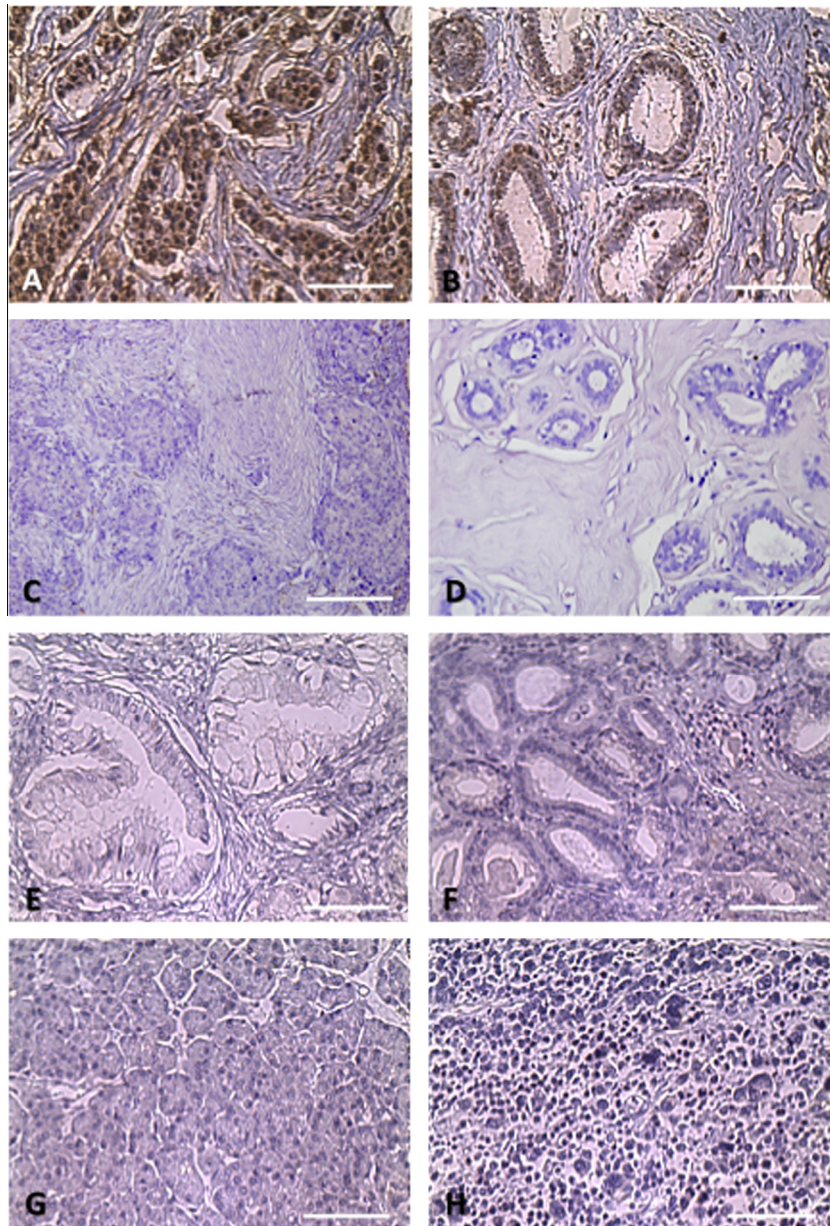


Fig. 6. Immunoaffinity of FAbC4 against breast cancer tissue antigens. (A) Invasive adenocarcinoma showing striking labeling in the nucleus and cytoplasm from ductal cells. (B) Moderate cytoplasmic immunoreactivity of ductal epithelial cells in benign breast tissue with fibroadenoma. (C) Mamoplasty sample tissue showing none labeling with FAbC4. (D) Negative control of immunohistochemistry assay. (E–H) None immunoreactivity was observed in other cancer types, such as prostate, stomach, pancreas and lymphoma. Counterstaining: Hematoxylin. Magnification: 200 \times .

100 μ L of each culture supernatant were added to appropriate wells and incubated at room temperature for 2 h. The plates were washed 5 times with PBST. HRP-conjugated rat anti-HA antibody was added to each well (100 μ L, 1:1000 dilution) and the plates were incubated 1 h at room temperature. The plates were washed 5 more times with PBST and revealed with 100 μ L of o-phenylenediamine substrate (Sigma Aldrich). Reactions were stopped with 4 N of sulfuric acid, and the absorbances read at 450 nm.

2.9. Purification of soluble antibodies

The TOP10 *E. coli* non-suppressor strain was transformed with the positive clone determined by ELISA, and used to inoculate SB culture containing 50 μ g/mL of carbenicillin and 2% glucose, which was grown under agitation at 37 $^{\circ}$ C overnight. Then, 2 mL were diluted in 200 mL of supplemented carbenicillin SB medium, and incubated for 6–8 h under agitation (250 rpm) at 37 $^{\circ}$ C, followed by a centrifugation at 3000 \times g for 10 min at 4 $^{\circ}$ C. Bacteria were resuspended in 1000 mL in supplemented carbenicillin SB medium, and induced with 2.0 mM IPTG at 30 $^{\circ}$ C overnight. The cultures were then centrifuged at 3000 \times g for 20 min to pellet bacterial cells. The supernatant was used for purification of Fab

soluble antibodies by HPLC (Amersham Biosciences) according to the manufacturer's instructions. Positive fractions were pooled and their concentrations were obtained spectrophotometrically by absorbance readings at 260 (A1) and 280 nm (A2) according to the following formula: [protein] = $K3 \times A2 - K4 \times A1$; where $K3 = 1552$, and $K4 = 757.3$. The samples were desalted by a Centriprep column, lyophilized and resuspended in PBS/BSA1%.

2.10. Sequence analysis

Phagemid DNA from positively selected clones and from the original library was sequenced using the MegaBACE 1000 automatic sequencer (Molecular Dynamics). The sequencing reactions were prepared with specific reverse primers MMB5 (5' CGTTTGCCATCTTTTCATAATC 3') for VH and MMB4 (5' GCTTCCGCTCGTATGTTGTGT 3') for V κ genes. V gene sequence determinations were based on Phred base calling [25] and chromatograms were used for manual verification of sequence ambiguities. Sequence alignments and translations were made with the program BlastX. V gene families were assigned using the Ig-Blast ser-

Table 2
FabC4 expression detected by immunohistochemistry in breast tumor samples and the clinical-histopathological variables (N = 232).

Variable	N	FabC4		P-Value
		Negative N (%)	Positive N (%)	
Age (years)				0.04^a
<40	34	6 (17.6)	28 (84.2)	
40–60	110	33 (30.0)	77 (70.0)	
>60	88	32 (36.4)	56 (63.6)	
Menopausal status				0.77
Pre	98	29 (29.6)	69 (70.4)	
Post	134	42 (31.3)	92 (68.7)	
ER				0.09
Positive	134	46 (34.3)	88 (65.7)	
Negative	84	20 (23.8)	64 (76.2)	
PgR				0.01
Positive	93	37 (39.8)	56 (60.2)	
Negative	127	30 (23.6)	97 (76.4)	
HER-2				1.00 ^b
Positive	22	6 (27.3)	16 (72.7)	
Negative	166	49 (29.5)	117 (70.5)	
Histological grading				<0.001
GI	44	18 (40.9)	26 (59.1)	
GII	127	46 (36.2)	81 (63.8)	
GIII	61	7 (11.5)	54 (88.5)	
Breast cancer subtypes				0.05
ER-/PgR-/HER-2-	48	9 (18.8)	39 (81.3)	
ER-/PgR-/HER-2+	16	3 (18.8)	13 (81.3)	
Luminal	148	52 (35.1)	96 (64.9)	
Tumor size (cT)				0.24
T ₁	19	6 (31.6)	13 (68.4)	
T ₂	101	35 (34.7)	66 (65.3)	
T ₃	8	9 (18.8)	39 (81.3)	
T ₄	64	21 (32.8)	43 (67.2)	
Lymph node (cN)				0.26
N ₀	74	19 (25.7)	55 (74.3)	
N ₁₋₃	158	52 (32.9)	106 (67.1)	
Distant metastasis (cM)				1.00
M ₀	212	65 (30.7)	147 (69.3)	
M ₁	20	6 (30.0)	14 (70.0)	
Recurrence				0.30
Yes	118	33 (28.0)	85 (72.0)	
No	111	38 (34.2)	73 (65.8)	
Death				0.16
Yes	113	30 (26.5)	83 (73.5)	
No	117	41 (35.0)	76 (65.0)	
Breast cancer	232	71 (30.6)	161 (69.4)	0.0002^a
Benign breast disease	34	21 (61.8)	13 (38.2)	
Ovary cancer	3	3 (100.0)	0	
Lymphoma	3	3 (100.0)	0	
Pancreas	3	3 (100.0)	0	
Prostate	3	3 (100.0)	0	
Stomach	3	3 (100.0)	0	

Significant values (P < 0.05) are in bold.

HER-2, human epidermal growth factor receptor-2; ER, estrogen receptor; PgR, progesterone receptor.

^a Chi-square for trend.^b Fisher exact test.

ver at NCBI (<http://www.ncbi.nlm.nih.gov>). Complementary determining (CDR) and framework region assignments were based on Kabat definition (www.bioinf.org.uk/abs/). Only high quality sequences were used for translation.

2.11. Immunohistochemistry

After Fab selection, the affinity of mammary tissue epitopes was verified by immunohistochemical localization. Additional samples of breast adenocarcinoma, breast fibroadenoma and normal breast from mamoplasties were processed and submitted to immunohistochemistry analyses, which were carried out by the following steps: sections were incubated with citrate buffer 6 M for 1 h at 90 °C for antigen retrieval. The peroxidase blockage was performed with H₂O₂ 3% in water for 30 min followed by blockage of unspecified sites with PBS/BSA 10% for 1 h at room temperature. Then, the Fab addition (1:25) in tissue sections was sequentially performed at 4 °C overnight. Control sections were incubated only with PBS. Immunofluorescence was analyzed by a mouse anti-HA conjugated to horseradish peroxidase (Sigma, 1:200 in PBS) for 1 h at room temper-

ature. Slides were then revealed with diaminobenzidine substrate solution, counterstained with hematoxylin and observed in a light microscope (Olympus BX40). The photomicrographs were made by the *software* HLImage (Western Vision Software, USA).

2.12. Immunoprecipitation and protein sequencing

We performed immunoprecipitation of FabC4 using Mouse Anti-His mAb Mag Beads (GenScript) according to manufacturer's instructions. Bound proteins were precipitated out of solution using the ProteoExtract kit (Calbiochem) and the protein pellet was left to dry overnight in a sterile fumehood. The lyophilized pellet was then resuspended in 50 mM Ammonium bicarbonate (pH 8.0) and subjected to an in-solution tryptic digestion (Mike Myers, Cold Spring Harbor modified by Brett S. Phinney, UC Davis Proteomics Core). Digested peptides were then de-salted using aspire tips (Thermo-Fisher Scientific, RP30 tips) before being resuspended in loading buffer.

Digested peptides were analyzed using a LTQ-FT (Thermo Fisher Scientific) coupled with a MG4 paradigm HPLC (Michrom, Auburn, CA). The samples were loaded onto a Michrom cap trap (0.5 × 2 mm) to be de-salted. The peptides were then separated using a Michrom Magic C18AQ (200 μm × 150 mm) reversed-phase column, and eluted using a gradient during a period of 60 min. Collision induced dissociation was applied to the peptide samples and data was acquired with an isolation width of 1, a normalized collision energy of 35 and a resolution of 50,000. The spray voltage on the Michrom captive spray was set to 1.8 kV with a heated transfer capillary temperature of 200 °C.

Raw data was analyzed using XTandem and visualized using Scaffold (Proteome Software, version 3.01). Samples were searched against Uniprot human (130,611 sequences) database appended with the cRAP (commonly found laboratory contaminants) and the reverse decoy databases.

2.13. Breast cancer sampling for Fab validation

To validate the FabC4, a population of BC patients' samples (N = 232) with long-term follow-up were obtained from A.C. Camargo Cancer Hospital (São Paulo, Brazil) and evaluated by immunohistochemistry in a previously constructed tissue microarray [26]. Patients were followed prospectively with a mean follow-up of 88.5 ± 63.1 months (3–227 months). All samples were from untreated patients before surgery. Patient's characteristics are described in Table 1.

2.14. Statistical analysis

The efficacy of selected clones in discriminating BC vs controls was tested by ELISA assays (in the absence of an arbitrary cutoff value). The data is summarized in ROC (receiver operating characteristic) curves, which were plotted by using the sensitivity (true positives) on the Y-axis against 1 – specificity (false positives) on the X-axis, considering each observed value as a possible cutoff value. The AUC (area under the curve) was calculated as a single measure for the discriminative efficacy of the marker. When a marker has no discriminative value, the ROC curve will lie close to the diagonal and the AUC is close to 0.5. When a test has strong discriminative value, the ROC curve will move up to the upper left-hand corner and the AUC will be close to 1.0. The chi-square test (or Fisher exact) was applied to determine the strength of association between the categorical variables. Disease-free survival (DFS) and overall survival (OS) probabilities were calculated using the Kaplan–Meier method. The end-point for OS analysis was restricted to death due to breast cancer, and the end-point for DFS analysis was distant metastasis diagnosis. Stage IV patients were excluded from these analyses. Kaplan–Meier survival curves for FabC4 were also calculated in BC patients stratified according to molecular profile status. Multivariate analysis was carried out using Cox proportional hazards model. The following variables were included in the multivariate model according to their biological context relating to BC: age, ER, PgR, HER-2, histological grade, cT, cN, chemotherapy, hormonal therapy, radiation treatment as well as the FabC4 status. Additionally, variables with a p-value < 0.2 in the univariate analyses also entered in the multivariate model. The statistical analyses were carried out using SPSS version 15.0 (SPSS; Chicago, IL) for Windows.

3. Results

3.1. Library characterization

Eighty V sequence regions were analyzed and, although all the clones in the library bear a full length insert, only 76% of them presented a functional VH/VL Fab fusion, resulting in a functional library size of 1.7 × 10⁶.

The variable regions were derived from nine different V gene families, including five VH gene families (VH1, VH2, VH3, VH4 and VH5) and four VL subgroups (Vκ1, Vκ3, Vκ4 and Vκ5). The

Table 3
Disease-free survival and overall survival analyses of TNM stage I–III triple negative breast cancer patients (N = 42).

Variable	N	DFS		P	OS		P*
		5 years (%)	10 years (%)		5 years (%)	10 years (%)	
Age (years)				0.652			0.691
<40	8	37.5	37.5		37.5	37.5	
40–60	24	52.9	36.1		57.4	41.8	
>60	10	30.0	30.0		30.0	30.0	
Menopausal status				0.636			0.667
Pre	24	40.0	31.1		44.1	35.3	
Post	18	50.0	42.9		50.0	42.9	
Histological grading				0.872			0.950
G1	1	100	0.0		100	0.0	
G2	19	41.4	41.4		46.3	40.5	
G3	22	44.1	33.0		43.5	38.0	
Tumor size (cT)				0.019			0.054
T ₁	4	25.0	25.0		25.0	25.0	
T ₂	14	55.6	46.3		53.4	44.5	
T ₃	15	53.3	53.3		60.0	52.5	
T ₄	9	22.2	0.0		22.2	11.1	
Lymph node (cN)				0.320			0.333
N ₀	12	54.7	41.0		53.5	53.5	
N _{1–3}	30	40.0	32.3		42.9	31.7	
EGFR				0.568			0.503
Positive	4	50.0	50.0		50.0	50.0	
Negative	36	46.5	35.3		48.7	26.9	
CK5/6				0.655			0.682
Positive	9	44.4	44.4		38.9	38.9	
Negative	32	46.7	36.1		49.8	28.8	
P63				0.068			0.095
Positive	6	16.7	16.7		16.7	16.7	
Negative	35	53.6	39.1		52.7	42.3	
FabC4				0.010			0.020
Positive	34	51.8	40.3		51.2	43.8	
Negative	8	12.5	12.5		25.0	12.5	

Significant values are in bold.

DFS, disease-free survival; OS, overall survival.

* P-Values obtained by log-rank test.

VH and VL repertoire are represented in Fig. 2. A slight predominance of the VH3 family with no Vk2 amplification was observed, and VH and VL sequences of CDR3 were highly diverse. Thus, the Fab gene fragments were distributed across the full repertoire of antibody germline genes.

Among selected clones, 98% of them encoded full-length, functional Fab molecules as determined by slot-blot and sequencing analyses (data not shown). In the slot-blot analysis, the presence of Fab in the induced culture supernatants was detected using HRP-conjugated anti-HA-HRP (Fig. 3A). Out of 95 clones tested, 93 showed a positive signal. In order to confirm the presence of Fab fragments, four randomly selected induced supernatants were separated by SDS-PAGE under reduced conditions and blotted onto nitrocellulose membrane. Detection of heterologous immunoglobulin was demonstrated by HRP-conjugated monoclonal anti-HA antibody immunostaining. The complex profile observed in SDS-PAGE may indicate bacterial lyses during culturing due to the Fab toxicity (Fig. 3B). As expected, the Fab presented a calculated molecular mass of 56 kDa, which is a result of the disulfide bond dissociation in reduced conditions, generating two 28-kDa chains, as demonstrated by the western blot analysis (Fig. 3C). Sequencing analysis revealed different sequences for these induced clones.

3.2. ELISA screening and purification of the selected clone

The specificity of the selected soluble Fab's against breast cancer antigens was determined by ELISA assays. Eight clones demonstrated differential reactivity to the pool of proteins extracted from normal, benign tumor and breast cancer tissues (Fig. 4A). All of them discriminated, by ANOVA test, benign from breast cancer

tissues. Only the D12 clone could not differentiate normal from BC samples. Nevertheless, only the FabC4 clone was selected for further analyses, based on its highest reactivity ratios between cancer/benign and cancer/normal (Fig. 4B). No positive signal was observed in the negative control (pComb3X without insert).

The selected clone was amplified and its phagemid was used to transform TOP10 *E. coli* non-suppressor strain, which was required to express soluble Fab molecules without the fused pIII protein and in high concentrations for HPLC purification. After each sample fractionation, 500 µL of the eluted solution were collected. The tubes with the highest concentration were pooled and concentration was calculated by spectrophotometric readings. The yield of purified Fab was 0.3 g/L. Samples were desalted by a Centriprep column, lyophilized and resuspended in PBS/BSA1%.

3.3. FabC4 target identification and tissue microarray analysis

The antigen corresponding to the FabC4 antibody was characterized as Cytokeratin 10 (CK10) by immunoprecipitation experiments and mass spectrometry.

In order to characterize the FabC4 binder, we have performed a magnetic capture to both breast tumor and benign tissue antigens with the conjugated FabC4 to magnetic nanoparticles. This immunoprecipitation was submitted to mass spectrometry analysis, which was interpreted by removing the most prevalent contaminants, such as hemoglobin, albumin and actin. To restrict the number of putative targets, we have set 20% protein coverage with at least 10 peptide matches per target in tumor tissues. We have used the immunohistochemistry staining intensity for both groups to validate the proportion observed in the protein coverage and

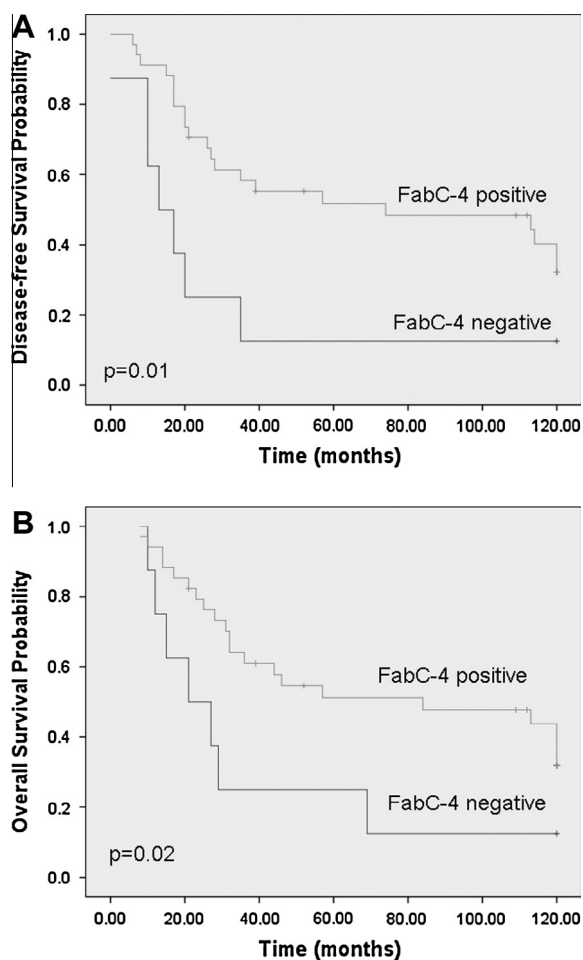


Fig. 7. Disease-free survival and overall survival curves according to FabC4 immunoreactivity. *P* values were determined by log-rank test.

peptide matches (3:1), by comparing tumor versus benign tissues. For tumor tissues, we detected three potential targets (CK1, CK9 and CK10), which were also observed in benign tissues, but in different proportions (Fig. 5). Since CK1 (Fig. 5A) and CK10 (Fig. 5C) form a heterodimer and they were the most prevalent in tumor tissues with the highest matches, we discarded the CK9 (Fig. 5B) as a target. CK1 was additionally eliminated from our potential target due to its greater coverage and number of peptide matches observed in benign tissues, a result incompatible with the immunohistochemistry data. Therefore, a recombinant CK10 (Abnova) was obtained and submitted to ELISA with FabC4, which showed a strong positive reactivity, similar to the reaction observed for BC tissue proteins and significantly different ($P < 0.01$) from expression levels found in the other two groups (Fig. 4C). Evidences also suggest that the specific ligand of the FabC4 antibody is a conformational epitope of the CK10, as shown by negative western blot and positive ELISA results (data not shown).

Immunohistochemistry data of the FabC4 is also displayed in Fig. 6. Immunostaining was significantly higher ($P = 0.0002$) in BC compared to benign tumor, and increased expression levels were correlated with the invasive breast cancer tumors in comparison to benign and normal breast tissues. Strong labeling was observed in the ducts of invasive carcinoma (Fig. 6A), while the benign section showed a moderate immunoreactivity (Fig. 6B), and no labeling was observed in normal breast tissue (Fig. 6C) and reaction control sections (Fig. 6D). Moreover, no or weak cross-reactions of the FabC4 with other cancer tissue types, such as prostate, stomach, pancreas and lymphoma were observed (Fig. 6E–H).

3.4. FabC4 immunoreactivity in breast cancer and clinical-histopathological variables

Negative association between age at diagnosis and FabC4 immunoreactivity rates was observed ($P = 0.04$), since 84.2% of BC patients <40 years had FabC4 expression in comparison with 63.6% of positivity from BC patients >60 years old (Table 2). Patients with absence of ER and PgR expression had higher percentage of FabC4 positivity, although only PgR analysis reached statistical significance ($P = 0.09$ and $P = 0.01$, respectively, Table 2). Histological grades were clearly associated with FabC4, since its positivity rates were 59.1%, 63.8%, and 88.5% in GI, GII, and GIII BCs, respectively ($P < 0.001$, Table 2). Regarding the molecular profile classification, luminal BCs presented lower FabC4 immunoreactivity in comparison with non-luminal tumors. On the other hand, we could not observe any difference between Her2-enriched and TNBC (Table 2). Regarding menopausal status, HER-2 protein expression, and initial TNM stage, no statistical significant associations were observed (Table 2).

3.5. FabC4 immunoreactivity and breast cancer outcomes

No association was observed between FabC4 immunoreactivity and DFS and OS analysis. As expected, significant associations were detected between the clinical outcome and the established prognostic factors (nodal status, clinical stage, histological grade, ER and PgR status, and molecular profile).

Multivariate analysis demonstrated that tumor size (cT) and lymph node status (cN) were the only independent prognostic factors for DFS (HR: 1.80; 95% CI: 1.36–2.26; $P < 0.001$ and HR: 2.20; 95% CI: 1.26–3.75; $P = 0.005$, respectively). Regarding OS, in addition to cT (HR: 1.7; 95% CI: 0.27–2.16; $P < 0.001$) and cN (HR: 1.9; 95% CI: 0.09–3.34; $P = 0.023$), histological grade also presented independent prognostic impact (HR: 1.50; 95% CI: 0.03–2.18; $P = 0.032$).

BC patients were stratified according to immunohistochemical subtypes (luminal vs. HER2-enriched vs. TNBC) and Kaplan–Meier survival curves were calculated. No prognostic impact was observed regarding the FabC4 status in the groups of luminal and also in the HER2-enriched BCs (data not shown).

However, in the group with TNBCs, FabC4 status could differentiate cases with distinct outcomes. Tumors with FabC4 expression showed significantly increased DFS and OS ($P = 0.01$ and $P = 0.02$, respectively, Table 3 and Fig. 7). The median DFS of TNBCs was 13 months and 74 months in the groups with negative and positive FabC4, respectively. Furthermore, median OS was 21 months and 84 months, in the groups with negative and positive FabC4, respectively.

Multivariate analysis on the TNBC cases ($N = 42$) demonstrated that FabC4 status is an independent prognostic factor for DFS and probably for OS. Lower risk of metastasis due to the disease was observed in FabC4-positive tumor patients (HR = 0.146, 95% CI 0.042–0.514, $P = 0.003$), and also those submitted to radiotherapy (HR = 0.151, 95% CI 0.036–0.643, $P = 0.011$). On the other hand, patients submitted to chemotherapy (HR = 6.567, 95% CI 1.407–30.649, $P = 0.017$) and those with tumors expressing the P63 protein (HR = 8.596, 95% CI 1.197–33.638, $P = 0.002$) presented lower DFS. Regarding OS, the only variable retained in the final model was radiotherapy (HR = 0.283, 95% CI 0.081–0.991, $P = 0.048$).

4. Discussion

Breast cancer (BC) is a heterogeneous disease, encompassing a wide variety of histological types and clinical behaviors. Current histological classification systems for breast cancer are based on

descriptive entities that are of prognostic significance. Since few predictive biomarkers are currently available, we have used the phage display technology and a newly constructed Fab antibody combinatorial library from breast cancer tissues to select a novel antibody that was not only capable of improving BC diagnosis, but could also be used as for prognostics, which to our best of knowledge there is no such a marker [3]. Most important, only recently [27] two tissue biomarkers (ubiquitin and truncated S100P) were used in combination to discriminate breast cancer from healthy tissues, but the publication failed to present any diagnostic parameter (sensitivity and specificity).

We have successfully selected a reactive antibody, FabC4, with good sensitivity (70%) and specificity (62%) for diagnosis, good correlation with disease staging due to its increased expression during disease progression, and association with a subset of triple negative BCs with good prognosis. The FabC4 targets the Cytokeratin 10 (CK10) protein, and the determinant region seems to be recognized as a specific conformational epitope in breast cancer.

The FabC4–ligand is breast specific, and its presence in some patients with benign diseases may be an indication of a pre-neoplastic disease without significant morphology alterations. On the other hand, the absence of the biomarker in tumor tissues may be due to the heterogeneity of the disease and some of the alterations cannot be explained by post-translational modifications of the CK10.

The possible recognition of a CK10 conformational epitope raises a fundamental question whether CK10 post-translational modifications may present different biological roles in breast cancer. This interfilament can bind to several other proteins, such as protein kinases (PKC, PKB) and Akt, which can regulate the cell cycle machinery, and present specific interactions in breast cancer. The role of the cytokeratins, including CK10, has no long been thought to be only structural, as this single function does not explain their diverse tissue and specific expression patterns [28,29].

This is the first potential biomarker for breast cancer diagnosis and histological classification linked to a CK10 epitope. Interestingly, CK10 has been associated with other cancers, and is one of the most common proteins in lymphatic metastases of cancers revealed by proteomic and protein functional studies [30]. CK10 has also been associated with poor prognosis in hepatocellular carcinoma regardless of tumor-node-metastasis stage, and vascular invasion [31] and with invasive carcinomas, in which the expression of keratin 10 was significantly associated with keratinizing carcinomas [32]. But because of the high specificity found in breast tissues in our study, we cannot rule out the possibility that conformational changes in CK10 may be associated with loss of function, as demonstrated in a CK10-null mouse model elsewhere [33], which has shown that CK10 is downregulated in squamous cell carcinomas and it is absent in proliferating cells *in vivo*, linking CK10 functions to both cellular architecture and cell cycle control. At present, a causal role in tumorigenesis is not established for any keratin, and additional studies must be done to elucidate CK10 function in breast cancer. Furthermore, the identification of keratin associated proteins and the analysis of keratin phosphorylation are beginning to provide insights into the molecular mechanisms by which they act, once reorganization of keratin IFs in response to extra- or intracellular signals predominantly involves phosphorylation events [34].

Phage antibody library has been used before to generate high-affinity antibodies against previously defined tumor-associated antigens such as-CEA and c-erb-2 [35–37], but were performed against specific ligands, different from our subtractive approach with unknown antigen target, which resulted in several tissue markers. The selected FabC4 presented an overall accuracy of

61%, but its expression was increased during cancer development and reached a positivity of 88.5% in advanced BC stages.

Because our antibody showed a gradual immunoaffinity according to histopathological grade of mammary gland ducts with invasive carcinoma, and the CK10 epitope ligand showed significant protein expression in tumor tissues when compared to benign and normal tissues, it is expected that CK10 may also show differential expression during cancer progression with high tissue immunoreactivity to undifferentiated ducts, and weak or no reactivity to differentiated ducts from infiltrative adenocarcinoma or normal tissue from mammoplasty. The low expression in normal tissues may be due to the lack of post-translational modifications, which may play a critical role in the malignant transformation.

Challenging situations of metastatic cancers with unknown primary is very common, and deserves the utilization of breast-specific markers for differentiating BC from non-breast tissues. In this sense, ER, mammaglobin and gross cystic disease fluid protein-15 (GCDFP-15) are widely accepted biomarkers for immunohistochemistry [38]. Cases of metastatic TNBC are even more difficult for the pathologist, since those markers are less expressed [39].

ER, PR, HER-2, and Ki-67 protein expression are routinely evaluated in order to classify BCs into different subtypes, namely luminal A, luminal B, HER-2-enriched and TNBC [40]. Though widely used in clinical practice these biomarkers are not capable to capture the complexity of BC. TNBC represents a subset of aggressive tumors accounting for 15% to 20% of newly diagnosed BC cases [41]. Potential therapeutic targets are likely to be identified while the heterogeneity of TNBC is better defined [42]. In the present study, FabC4 clone was associated with more aggressive tumors; i.e., those younger patients, with lack of PgR expression, higher histological grades and non-luminal BCs. Interestingly, in the subset of known aggressive TNBCs, FabC4 was a good prognostic marker.

The major limitation of our study is regarding the sub-analysis of FabC4 prognostic impact in TNBCs, since the number of patients evaluated was very small. However, it was observed a very low hazard rate for DFS (HR = 0.146) after multivariate analysis. Even considering the possible bias related to the small sample size, our findings suggest that the prognostic impact of FabC4 merits further evaluation in the TNBC patients.

In conclusion, the CK10-epitope specific Fab antibody is the first diagnostic and prognostic specific breast tissue biomarker, which can be used for BC diagnosis and staging, and it was also associated with a subset of triple negative BCs with good prognosis. Its role in BCs should be addressed in future studies.

Conflict of Interest

We wish to confirm that there are no known conflicts of interest associated with this publication and there has been no significant financial support for this work that could have influenced its outcome. We confirm that the manuscript has been read and approved by all named authors and that there are no other persons who satisfied the criteria for authorship but are not listed. We further confirm that the order of authors listed in the manuscript has been approved by all of us.

We confirm that we have given due consideration to the protection of intellectual property associated with this work and that there are no impediments to publication, including the timing of publication, with respect to intellectual property. In so doing we confirm that we have followed the regulations of our institutions concerning intellectual property.

We further confirm that any aspect of the work covered in this manuscript that has involved human patients has been conducted with the ethical approval.

Acknowledgements

The authors would like to thank the financial support by CNPq, CAPES, Ministry of Health (Department of Science and Technology, DECIT) and FAPEMIG. We would like to thank the Histopathology Laboratory of the Federal University of Uberlândia for providing the immunohistochemistry assays. We are also grateful to Prof. Dr. Andréia Q. Maranhão (University of Brasília, Brazil) for providing the pComb3X vector.

References

- [1] C. DeSantis, R. Siegel, P. Bandi, A. Jemal, Breast cancer statistics, *CA Cancer J. Clin.* 61 (2011) (2011) 409–418.
- [2] D.M. Parkin, F. Bray, J. Ferlay, P. Pisani, Global cancer statistics, *CA Cancer J. Clin.* 55 (2005) (2002) 74–108.
- [3] F.C. Geyer, C. Marchio, J.S. Reis-Filho, The role of molecular analysis in breast cancer, *Pathology* 41 (2009) 77–88.
- [4] M. Latterich, M. Abramovitz, B. Leyland-Jones, Proteomics: new technologies and clinical applications, *Eur. J. Cancer* 44 (2008) 2737–2741.
- [5] A.M. Hanby, The pathology of breast cancer and the role of the histopathology laboratory, *Clin. Oncol. (R Coll Radiol)* 17 (2005) 234–239.
- [6] M. Popkov, C. Rader, C.F. Barbas 3rd, Isolation of human prostate cancer cell reactive antibodies using phage display technology, *J. Immunol. Methods* 291 (2004) 137–151.
- [7] P. Holliger, P.J. Hudson, Engineered antibody fragments and the rise of single domains, *Nat. Biotechnol.* 23 (2005) 1126–1136.
- [8] S.J. Kim, Y. Park, H.J. Hong, Antibody engineering for the development of therapeutic antibodies, *Mol. Cells* 20 (2005) 17–29.
- [9] T. Ben-Kasus, B. Schechter, M. Sela, Y. Yarden, Cancer therapeutic antibodies come of age: targeting minimal residual disease, *Mol. Oncol.* 1 (2007) 42–54.
- [10] P.S. Hall, D.A. Cameron, Current perspective – trastuzumab, *Eur. J. Cancer* 45 (2009) 12–18.
- [11] M. Hust, S. Dubel, Mating antibody phage display with proteomics, *Trends Biotechnol.* 22 (2004) 8–14.
- [12] P. Pansri, N. Jaruseranee, K. Rangnoi, P. Kristensen, M. Yamabhai, A compact phage display human scFv library for selection of antibodies to a wide variety of antigens, *BMC Biotechnol.* 9 (2009) 6.
- [13] A.D. Griffiths, S.C. Williams, O. Hartley, I.M. Tomlinson, P. Waterhouse, W.L. Crosby, R.E. Kontermann, P.T. Jones, N.M. Low, T.J. Allison, et al., Isolation of high affinity human antibodies directly from large synthetic repertoires, *EMBO J.* 13 (1994) 3245–3260.
- [14] H.M. Azzazy, W.E. Highsmith Jr., Phage display technology: clinical applications and recent innovations, *Clin. Biochem.* 35 (2002) 425–445.
- [15] G.P. Smith, V.A. Petrenko, Phage display, *Chem. Rev.* 97 (1997) 391–410.
- [16] H.J. de Haard, N. van Neer, A. Reurs, S.E. Hufton, R.C. Roovers, P. Henderix, A.P. de Bruine, J.W. Arends, H.R. Hoogenboom, A large non-immunized human Fab fragment phage library that permits rapid isolation and kinetic analysis of high affinity antibodies, *J. Biol. Chem.* 274 (1999) 18218–18230.
- [17] B.P. Wu, B. Xiao, T.M. Wan, Y.L. Zhang, Z.S. Zhang, D.Y. Zhou, Z.S. Lai, C.F. Gao, Construction and selection of the natural immune Fab antibody phage display library from patients with colorectal cancer, *World J. Gastroenterol.* 7 (2001) 811–815.
- [18] X. Cai, A. Garen, Anti-melanoma antibodies from melanoma patients immunized with genetically modified autologous tumor cells: selection of specific antibodies from single-chain Fv fusion phage libraries, *Proc. Natl. Acad. Sci. USA* 92 (1995) 6537–6541.
- [19] V.A. Somers, R.J. Brandwijk, B. Joosten, P.T. Moerkerk, J.W. Arends, P. Menheere, W.O. Pieterse, A. Claessen, R.J. Scheper, H.R. Hoogenboom, S.E. Hufton, A panel of candidate tumor antigens in colorectal cancer revealed by the serological selection of a phage displayed cDNA expression library, *J. Immunol.* 169 (2002) 2772–2780.
- [20] P.J. Mintz, J. Kim, K.A. Do, X. Wang, R.G. Zinner, M. Cristofanilli, M.A. Arap, W.K. Hong, P. Troncoso, C.J. Logothetis, R. Pasqualini, W. Arap, Fingerprinting the circulating repertoire of antibodies from cancer patients, *Nat. Biotechnol.* 21 (2003) 57–63.
- [21] Q. Zhang, S.H. Zhang, M.Q. Su, G.Q. Bao, J.Y. Liu, J. Yi, J.J. Shen, X.K. Hao, Guided selection of an anti-gamma-seminoprotein human Fab for antibody directed enzyme prodrug therapy of prostate cancer, *Cancer Immunol. Immunother.* 56 (2007) 477–489.
- [22] J.D. Marks, H.R. Hoogenboom, T.P. Bonnert, J. McCafferty, A.D. Griffiths, G. Winter, By-passing immunization. Human antibodies from V-gene libraries displayed on phage, *J. Mol. Biol.* 222 (1991) 581–597.
- [23] P. Chomczynski, N. Sacchi, Single-step method of RNA isolation by acid guanidinium thiocyanate-phenol-chloroform extraction, *Anal. Biochem.* 162 (1987) 156–159.
- [24] J. Andris-Widhopf, P. Steinberger, R. Fuller, C. Rader, C. Barbas, Generation of antibody libraries: PCR amplification and assembly of light-and heavy-chain coding sequences, in: *Phage Display Laboratory Manual*, Cold Spring Harbor Laboratory Press, New York, 2001, pp. 9.1–9.22.
- [25] B. Ewing, P. Green, Base-calling of automated sequencer traces using phred. II. Error probabilities, *Genome Res.* 8 (1998) 186–194.
- [26] M.A. Nagai, J.H. Fregnani, M.M. Netto, M.M. Brentani, F.A. Soares, Down-regulation of PHLDA1 gene expression is associated with breast cancer progression, *Breast Cancer Res. Treat.* 106 (2007) 49–56.
- [27] L. Chung, S. Shibli, K. Moore, E.E. Elder, F.M. Boyle, D.J. Marsh, R.C. Baxter, Tissue biomarkers of breast cancer and their association with conventional pathologic features, *Br. J. Cancer* 108 (2013) 351–360.
- [28] J.M. Paramio, J.L. Jorcano, Beyond structure: do intermediate filaments modulate cell signalling?, *BioEssays: News Rev Mol., Cell. Dev. Biol.* 24 (2002) 836–844.
- [29] M.B. Omary, N.O. Ku, G.Z. Tao, D.M. Toivola, J. Liao, “Heads and tails” of intermediate filament phosphorylation: multiple sites and functional insights, *Trends Biochem. Sci.* 31 (2006) 383–394.
- [30] J. Zong, C. Guo, S. Liu, M.Z. Sun, J. Tang, Proteomic research progress in lymphatic metastases of cancers, *Clin. Transl. Oncol.* 14 (2012) 21–30.
- [31] X.R. Yang, Y. Xu, G.M. Shi, J. Fan, J. Zhou, Y. Ji, H.C. Sun, S.J. Qiu, B. Yu, Q. Gao, Y.Z. He, W.Z. Qin, R.X. Chen, G.H. Yang, B. Wu, Q. Lu, Z.Q. Wu, Z.Y. Tang, Cytokeratin 10 and cytokeratin 19: predictive markers for poor prognosis in hepatocellular carcinoma patients after curative resection, *Clin. Cancer Res.* 14 (2008) 3850–3859.
- [32] C. Carrilho, M. Albrero, L. Buane, L. David, Keratins 8, 10, 13, and 17 are useful markers in the diagnosis of human cervix carcinomas, *Human Pathol.* 35 (2004) 546–551.
- [33] J. Relchelt, T.M. Magin, Hyperproliferation, induction of c-Myc and 14-3-3 sigma, but no cell fragility in keratin-10-null mice, *J. Cell Sci.* 115 (2002) 2639–2650.
- [34] T.M. Magin, P. Vijayaraj, R.E. Leube, Structural and regulatory functions of keratins, *Exp. Cell Res.* 313 (2007) 2021–2032.
- [35] R. Schier, J. Bye, G. Apell, A. McCall, G.P. Adams, M. Malmqvist, L.M. Weiner, J.D. Marks, Isolation of high-affinity monomeric human anti-c-erbB-2 single chain Fv using affinity-driven selection, *J. Mol. Biol.* 255 (1996) 28–43.
- [36] R.H. Begent, M.J. Verhaar, K.A. Chester, J.L. Casey, A.J. Green, M.P. Napier, L.D. Hope-Stone, N. Cushen, P.A. Keep, C.J. Johnson, R.E. Hawkins, A.J. Hilson, L. Robson, Clinical evidence of efficient tumor targeting based on single-chain Fv antibody selected from a combinatorial library, *Nat. Med.* 2 (1996) 979–984.
- [37] J.K. Osbourn, A. Field, J. Wilton, E. Derbyshire, J.C. Earnshaw, P.T. Jones, D. Allen, J. McCafferty, Generation of a panel of related human scFv antibodies with high affinities for human CEA, *Immunotechnology* 2 (1996) 181–196.
- [38] R. Bhargava, S. Beriwal, D.J. Dabbs, Mammaglobin vs GCDPF-15: an immunohistological validation survey for sensitivity and specificity, *Am. J. Clin. Pathol.* 127 (2007) 103–113.
- [39] B.C. Litztenburger, C.J. Creighton, A. Tsimelzon, B.T. Chan, S.G. Hilsenbeck, T. Wang, J.M. Carboni, M.M. Gottardis, F. Huang, J.C. Chang, M.T. Lewis, M.F. Rimawi, A.V. Lee, High IGF-IR activity in triple-negative breast cancer cell lines and tumorgrafts correlates with sensitivity to anti-IGF-IR therapy, *Clin. Cancer Res.* 17 (2011) 2314–2327.
- [40] A. Goldhirsch, W.C. Wood, A.S. Coates, R.D. Gelber, B. Thurlimann, H.J. Senn, Strategies for subtypes—dealing with the diversity of breast cancer: highlights of the St. Gallen international expert consensus on the primary therapy of early breast cancer 2011, *Ann. Oncol.* 22 (2011) 1736–1747.
- [41] K.R. Bauer, M. Brown, R.D. Cress, C.A. Parise, V. Caggiano, Descriptive analysis of estrogen receptor (ER)-negative, progesterone receptor (PR)-negative, and HER2-negative invasive breast cancer, the so-called triple-negative phenotype: a population-based study from the California cancer Registry, *Cancer* 109 (2007) 1721–1728.
- [42] O. Metzger-Filho, A. Tutt, E. de Azambuja, K.S. Saini, G. Viale, S. Loi, I. Bradbury, J.M. Bliss, H.A. Azim Jr., P. Ellis, A. Di Leo, J. Baselga, C. Sotiriou, M. Piccart-Gebhart, Dissecting the heterogeneity of triple-negative breast cancer, *J. Clin. Oncol.* 30 (2012) 1879–1887.